Zhuo, L., Dai, Q., & Han, D. (2015). Evaluation of SMOS soil moisture retrievals over the central United States for hydro-meteorological application. Physics and Chemistry of the Earth, 83-84, 146–155. DOI: 10.1016/j.pce.2015.06.002

Evaluation of SMOS soil moisture retrievals over the central United States for hydro-meteorological application

Lu Zhuo[1*], Qiang Dai[2] and Dawei Han[1]

[1]WEMRC, Department of Civil Engineering, University of Bristol, Bristol, UK

[2] Key Laboratory of Virtual Geographic Environment of Ministry of Education, School of Geography Science, Nanjing Normal University, Nanjing, China

***Corresponding author:**

Lu Zhuo

Water and Environmental Management Research Centre

University of Bristol

93-95 Woodland Road

Bristol, BS8 1US, UK

E-mail: lz7913@bristol.ac.uk or salasalazhuo@hotmail.com

Submission

Physics and Chemistry of the Earth

Abstract

Soil moisture has been widely recognized as a key variable in hydro-meteorological processes and plays an important role in hydrological modelling. Remote sensing techniques have improved the availability of soil moisture data, however, most previous studies have only focused on the evaluation of retrieved data against point-based observations using only one overpass (i.e., the ascending orbit). Recently, the global Level-3 soil moisture dataset generated from Soil Moisture and Ocean Salinity (SMOS) observations was released by the Barcelona Expert Center. To address the aforementioned issues, this study is particularly focused on a basin scale evaluation in which the soil moisture deficit is derived from a three-layer Xinanjiang model used as a hydrological benchmark for all comparisons. In addition, both ascending and descending overpasses were analyzed for a more comprehensive comparison. It was interesting to find that the SMOS soil moisture accuracy did not improve with time as we would have expected. Furthermore, none of the overpasses provided reliable soil moisture estimates during the frozen season, especially for the ascending orbit. When frozen periods were removed, both overpasses showed significant improvements (i.e., the correlations increased from $r = –0.53$ to $r = –0.65$ and from $r = –0.62$ to $r = –0.70$ for the ascending and descending overpasses, respectively). In addition, it was noted that the SMOS retrievals from the descending overpass consistently were approximately 11.7% wetter than the ascending retrievals by volume. The overall assessment demonstrated that the descending orbit outperformed the ascending orbit, which was unexpected and enriched our knowledge in this area. Finally, the potential reasons were discussed.

Keywords: hydro-meteorology, passive microwaves, NLDAS-2, soil moisture deficit, SMOS, ascending, descending, Xinanjiang (XAJ)

1. Introduction

Although soil moisture comprises only 0.01% of the total amount of water on the earth (Prigent et al., 2005), the existence of soil moisture is significant for many application areas such as agriculture, meteorology, and climate investigations (Beljaars et al., 1996; Dai et al., 2004; Jung et al., 2010; Koster et al., 2004; Ookouchi et al., 1984; Seneviratne et al., 2010; Suseela et al., 2012; Wang and Qu, 2009; Yeh et al., 1984). In addition, there is abundant evidence that hydrological processes are significantly conditioned by a river basin's antecedent wetness state (Brocca et al., 2008; Western and Grayson, 1998). Many studies have shown that the distribution of a basin's water is influenced by soil moisture storage, with runoff generated instantaneously when a certain storage threshold is reached (Latron and Gallart, 2008; Spence, 2010; Tromp-van Meerveld and McDonnell, 2006). Therefore, monitoring soil moisture accurately is important in stream forecasting. Although land surface models have been able to produce global soil moisture information, they tend to be deficient owing to their lack of access to reliable data on soil and vegetation properties and atmospheric forcing as well as the time drift problem (i.e., accumulation of errors) (Collow et al., 2012). Conventional point-based observations are currently limited to discrete measurements at particular locations because the cost of direct observation of soil moisture over a large number of sites is very high (Vinnikov et al., 1999). Furthermore, ground-based measurements of soil moisture are made at localized points—typically 0.0025 m^2—and are not suitable for basin-level studies (Al-Shrafany et al., 2013; Srivastava et al., 2013b; Walker et al., 2004; Wang and Qu, 2009).

Alternatively, satellite remote sensing techniques are a major tool in retrieving soil moisture information on a large scale (Engman and Chauhan, 1995) and are able to scan the entire earth daily and provide soil moisture observations globally (Kerr et al., 2001). In particular, the data acquired by microwave sensors, both active and passive, have been employed to provide detailed soil moisture variability in recent years (Calvet et al., 2011). The launch of the Soil Moisture and Ocean Salinity (SMOS) mission in November 2009 clearly reveals the significance and determination of the global scientific community to support an advanced soil moisture observation system from space. It has been indicated by Kerr et al. (2001) that SMOS was developed to have an error less than 0.04 m^3/m^3 and a spatial resolution better than 50 km. In addition to SMOS, there are other similar

missions, including the Advanced Microwave Scanning Radiometer on Earth Observing System (AMSR-E; from 6.9 to 89.0 GHz; (Njoku et al., 2003)), which operated on the AQUA satellite between 2002 and 2011, and the Scanning Multichannel Microwave Radiometer (SMMR; 6.63 GHz; (Reichle et al., 2004)). It is anticipated that those soil moisture datasets would provide accurate soil moisture information for hydrological modelling such as real-time flood forecasting.

SMOS makes both ascending (6 a.m. local solar time (LST)) and descending (6 p.m. LST) overpasses every three days, and the performance of both retrievals remains unclear (Dente et al., 2012; Jackson et al., 2012; Rowlandson et al., 2012; Sanchez et al., 2012). Based on the literature review, previous studies mainly focused on the downscaling, assimilation, and evaluation of the SMOS ascending overpass in order to minimize the observation error caused by the daytime soil drying effect and the impact of vertical soil-vegetation temperature gradients (Jackson et al., 2012; Lacava et al., 2012; Njoku et al., 2003; Piles et al., 2011; Srivastava et al., 2013b). There also exists a significant problem when evaluating coarse-resolution satellite soil moisture products with point-based measurements owing to the disparity of spatial scales between the two datasets (Jackson et al., 2010; Rudiger et al., 2011). Based on previous studies, no particular attention is given for their evaluation over a basin scale, particularly for hydrological applications. It is expected that satellite soil moisture measurements are more accurate in the hours near dawn when the soil profile has the most time to return to an equilibrium state from the previous day's fluxes (Jackson, 1980). Hence, based on this hypothesis, it is more likely to be true that ascending soil moisture measurements would have better performance than their descending counterparts (Jackson et al., 2012). In addition, based on evaporation demand, it is expected that soil would be wetter at night and drier during the day; in other words, the ascending pass should hold higher soil moisture values than the descending pass (Collow et al., 2012).

In this context, the objective of this paper is to appraise both ascending and descending observations of SMOS through the Xinanjiang (XAJ) model-derived soil moisture deficit (SMD) over the Pontiac basin in the central U.S. to determine whether there are any substantial differences between the two and to judge whether they are suitable for hydrological modelling. In particular, the study covers the period from January 1, 2010 to December

31, 2013, thereby allowing us to evaluate the capability of both overpasses to capture the transitions from dry to wet conditions as well as from frozen to unfrozen seasons. Moreover, the multiyear soil moisture records allow us to investigate the possible improvement of SMOS accuracy through time. This paper has the following structure. In Section 2, the study area, soil moisture datasets, and methodology for SMOS soil moisture evaluations are described. Section 3 presents the results and discussion. Finally, Section 4 draws the conclusion of this study.

2. Data and methodology

2.1 Study area and datasets

The Vermilion River at Pontiac (1500 km^2) is chosen as the study basin and is located in Illinois, which is in the central U.S. (40.878 °N, 88.636 °W). It is influenced primarily by a hot summer continental climate (Peel et al., 2007), and its land cover is predominantly cropland (Bartholomé and Belward, 2005; Hansen, 1998) on Mollisols (Webb et al., 2000). The average altitude of the catchment is 188 m MSL (mean sea level), and the average annual rainfall is 867 mm. The layout of the Pontiac basin is shown in Fig. 1 along with the location of its flow gauge, NLDAS-2 grids, and distribution of river networks.

The NLDAS-2 (Mitchell et al., 2004) precipitation (P) and evapotranspiration (ET) at 0.125° spatial resolution and daily temporal resolution (converted from an hourly resolution) are first processed as data inputs to the XAJ model. The ET is generated from NARR (North American Regional Reanalysis). The precipitation data are calculated from the temporal disaggregation of the gauged daily precipitation data from NCEP/CPC (National Centers for Environmental Prediction/Climate Prediction Center) with an orographic adjustment based on the monthly climatological precipitation of the parameter-elevation regressions on independent slopes model (PRISM) (Daly et al., 1994). As presented in Fig. 1, there are a total of 20 NLDAS-2 grid points/grids covering the Pontiac basin. Both ET and P datasets have been converted into one basin-scale dataset using the weighted average method for use in the lumped XAJ model (i.e., if a grid is completely in the catchment, it is counted as 1. If a grid partially covers the catchment (e.g., 20% of its grid area), it is counted as 0.2. All values are then added to become the

denominator, and the numerator comprises the sum of the products of individual grid counts and the grid ET/P value. The average ET and P of the catchment are thus derived. For the Pontiac basin, the USGS daily flow data from January 2010 to April 2011 has been used for the calibration of the XAJ model, and the period of May to December 2011 has been used for the validation purpose. The SMOS soil moisture dataset evaluated in this study is available for the period from January 2010 to December 2013 and is obtained from the SMOS Barcelona Expert Center (SMOS-BEC).

2.2 The SMOS product

The SMOS satellite was launched at the end of 2009 and has been providing soil moisture data for almost six years. SMOS acquires the brightness temperature at a frequency of 1.4 GHz (L-band), which is a function of the emissivity and therefore of near-surface soil moisture (approximately 5 cm). The spatial resolution of SMOS products is 35–50 km (Kerr et al., 2010; Kerr et al., 2001) with a soil moisture retrieval unit in m^3/m^3.

In this study, the SMOS-BEC (http://cp34-bec.cmima.csic.es) is used, which has been recently released with various temporal resolutions: daily, 3-day, 9-day, monthly, and annually. These products are generated in the NetCDF format on two types of grids: the ISEA 4H9 grid (Icosahedral Snyder Equal Area projection with aperture 4, resolution 9) with hexagonal cell shape (Pinori et al., 2008), which utilizes the same grid as the Level-2 product, and the EASE (Equal Area Scalable Earth) grid with a pixel size of ~25 km × 25 km. In this study, the daily soil moisture product with the EASE grid is used, because the EASE grid is more widely utilized. The main method implemented to retrieve surface soil moisture is the same as that employed by the European Space Agency (ESA) operational algorithm for generating standard Level-2 soil moisture products (Kerr et al., 2012). This study separates the two SMOS passes in order to determine whether there are any differences between them and which pass is more suitable for hydrological applications.

2.3 XAJ hydrological model

The XAJ model is employed as a rainfall-runoff simulation model in this study, because it is well known and capable of accounting for soil water content in the system with a suitable time step. Moreover, it provides easy

access to data inputs for use in hydrological modelling. In hydrology, SMD is an important indicator of soil water content, which represents the amount of water to be added to a soil profile in order to bring it to field capacity (Calder et al., 1983; Rushton et al., 2006). The SMD can be calculated using the following equation (Srivastava et al., 2013b):

$$SMD = FC - SMC \quad (1)$$

where FC is the field capacity, which is considered as the upper limit in hydrological modelling for soil moisture, and SMC is the soil moisture content.

It has been proved by numerous studies that the three-layer XAJ model is very practical in calculating SMD from hydrological forcing (Ren-Jun, 1992; Zhao et al., 1995; Zhuo et al., 2014). The model has been widely applied to a large number of basins across the globe (Khan, 1993; Wang, 1991; Zhao, 1992; Zhao et al., 1995; Zhuo et al., 2015). The XAJ model is a fairly general conceptual lumped rainfall-runoff model; its main concept is the runoff generation on repletion of storage, which indicates that runoff is not emerged until the soil water content of its aeration zone reaches the field capacity. The structure of the XAJ model comprises an evapotranspiration module, a runoff production module, and a runoff routing module. The model comprises three soil layers (upper, lower, and deep), which represent the three evapotranspiration components. The XAJ model requires only the areal mean P and ET as data inputs and the observed flow for model calibration and validation (Peng et al., 2002). The XAJ model has 17 parameters, which include seven runoff production parameters (*WUM*, *WLM*, *WDM*, *B*, *IMP*, *K*, *C*) and ten routing parameters (*SM*, *EX*, *KG*, *KSS*, *KKG*, *KKSS*, *CS*, *V*, *dX*, *L*). All 17 parameters are calibrated in this study by determining the optimal performance of the model (Zhao, 1980; Zhao, 1992). The flowchart of the XAJ model is shown in Fig. 2. The three-layer SMDs are generated to determine the effect of drying and wetting on the basin soil storage. In this study, only the surface SMD is utilized to evaluate the SMOS soil moisture observations. It is worth mentioning that some previous studies (Al-Shrafany et al., 2013; Srivastava et al., 2014; Srivastava et al., 2013a; Srivastava et al., 2013b) have reported SMOS soil moisture evaluations against single-layer hydrological models, which resulted in a scale mismatch during the comparison; this was because SMOS soil moisture is measured only at the top 5 cm of the soil whereas the thickness of a single-layer hydrological

model can be considerably large. For this reason, the use of the three-layer XAJ model provides a more scale-matched evaluation of the SMOS soil moisture retrievals. Because the spatial coverage of the XAJ model is the size of the whole basin, the generated SMD is representative of an area larger than the one covered by ground-based observations; this arguably avoids the issue of the spatial mismatch between the in-situ and remotely sensed data (Lacava et al., 2012).

2.4 Performance indicators

Several performance indicators are used to assess various aspects of the comparison. Nash-Sutcliffe Efficiency (*NSE*) (Nash and Sutcliffe, 1970) is used to assess the performance of the XAJ model, and two statistical indicators are computed between pairs of remotely sensed soil moisture data (SMOS ascending and descending) and the XAJ SMD—Pearson product moment correlation coefficient r and Spearman rank correlation coefficient r_{sp}. *NSE* is the most common and important performance measure used in hydrology, and it is calculated by the following equation:

$$NSE = 1 - \frac{\sum_{i=1}^{n}(y_i - x_i)^2}{\sum_{i=1}^{n}(x_i - \bar{x})^2} \quad (2)$$

where x_i represents the observed values and y_i represents the simulated values. n is the number of data pairs.

Pearson product moment correlation coefficient r is used to evaluate the linear relationship between two variables, which is defined as:

$$r = \frac{n(\sum x_i y_i) - (\sum x_i)(\sum y_i)}{\sqrt{[n\sum x_i^2 - (\sum x_i)^2][n\sum y_i^2 - (\sum y_i)^2]}} \quad (3)$$

Spearman rank correlation coefficient r_{sp} is a nonparametric method for evaluating the degree of correlation between two independent variables (Chen et al., 2013a). Owing to its ability to cope with nonlinear as well as linear correlation, it is used in addition to r for a more comprehensive comparison.

$$r_{sp} = 1 - \frac{6\sum_{i=1}^{n} d_i^2}{n^3 - n} \quad (4)$$

where d_i is the difference between ranks for each soil moisture data pair (x_i, y_i).

3. Results and discussion

3.1. SMD estimation from XAJ model forced by NLDAS-2 datasets

First, the surface SMD is generated by running the XAJ model. For the calibration of the XAJ model, the period from January 2010 to April 2011 is used, and the period from May 2011 to December 2011 is for validation. The calibration procedure focuses especially on the modelling of ET and the distribution of the total runoff (e.g., surface runoff, interflow, and groundwater) as well as good agreement between the modelled and observed flows. There are 17 parameters used for XAJ initialization, and the optimal values with their initialization values used in this study are shown in Table 1. The overall performance indicates an *NSE* value of 0.81 for the calibration and 0.80 during the validation, which indicates that the model is acceptable. In this study, the surface SMD generated from XAJ is selected as a benchmark given the fact that the XAJ is capable of simulating the hydrological processes in the basin, even though the model is calibrated using the river flow. Therefore, the XAJ-simulated SMD is hydrologically a reliable indicator of surface soil water content albeit in an inverse relationship. The time series plots of rainfall and flow during the calibration and validation periods are presented in Fig. 3. The modelling result reveals that the XAJ model tends to match the measured flow rather well whereas there is a slight overestimation of low flows during the calibration. However, during the validation period, there is an overestimation of the overall flow simulation. Presumably, this largely could be due to the methods used for model parameter identification or the deficiency of the model structure itself. For this comparison study, the relevant state variable in the XAJ model is the SMD. The SMD is important in distributing rainfall into different runoff components. If the SMD is small, then more surface runoff will be generated after a rainfall event, and the remainder goes to interflow and groundwater. It is clear that at some parts of the flow simulation, the model is incapable of calculating the nonlinear behavior of the hydrological processes. This is particularly evident in the

recession curves and low flows. Nevertheless, during most of the monitoring periods, the XAJ model performs relatively well, and both *NSE* values are sufficiently high ($NSE \geq 0.8$) for an acceptable hydrological model.

3.2 Comparison of the SMOS products and SMD

To assess the SMOS performance, the time series of the two satellite-observed soil moisture measurements (from the ascending and descending orbits) against XAJ SMD for the period from January 1, 2010 to December 31, 2013, are plotted in Fig. 4; additional variables such as ET and P are also illustrated. As shown in Fig. 4a, the temporal plots of both SMOS overpasses demonstrate a high variability with seasons and follow a strong seasonal cycle (ranging from 0.046 to 0.48 m^3/m^3 and from 0.043 to 0.58 m^3/m^3 for the ascending and descending overpasses, respectively) with peaks normally in winter when ET is at its lowest. The Pontiac basin is mainly covered by cropland subjected to frequent frozen soil events during winter periods. The surface soil is frozen at the beginning of November, and the soil moisture value falls suddenly from greater than 0.2 to less than 0.1 m^3/m^3. It then thaws at the end of February with an abrupt soil moisture increase. It is clear to see that owing to frozen soil, SMOS is not able to retrieve valid observations until late February; the case is even worse for the ascending overpass in 2011. In Fig. 4b, the rainfall pattern illustrates that summer is the rainiest season. However, owing to high temperatures and increased evaporative demands, soils progressively dry out from April to September. Although winter has the least rainfall, owing to the low ET, soils are near the field capacity until the middle of March for most of the year. It can be observed in Fig. 4a and b that for the XAJ-generated SMD, high ET can lead to significantly large SMDs (i.e., the soil is near the wilting point) if rainfall quantity is less than ET. However, when ET is reduced while rainfall wets the soil profile, a surging phenomenon can be seen. Generally speaking, the SMD and the two SMOS overpasses are highly responsive to ET and rainfall events, illustrating notable fluctuations over the entire period and swift, sharp response even to small rainfall events.

It is evident that at many oscillations, higher soil moisture values are observed in the descending pass with lower values in the ascending pass. Merely looking at the time series plots is insufficient for a full evaluation. Hence, the scatterplots are made between the descending and ascending soil moisture measurements. The investigation is conducted by dividing data into four separate years between 2010 and 2013. As shown in Fig. 5, the descending-

over-ascending-wetting ratio (DoAW ratio; i.e., the difference between the descending and ascending soil moisture measurements divided by the ascending soil moisture) in each year appears positive, which indicates that descending soil moistures are on average wetter than ascending retrievals, especially in 2011. As a result, the soil moistures from the descending orbit consistently are approximately 11.7% by volume wetter than the ascending retrievals. This result contradicts the supposition that soil moisture should be at its driest in the late afternoon because SMOS registers the opposite result, and similar results were discovered by Collow et al. (2012). This phenomenon could be explained by the effect of radio frequency interference (RFI) in this region.

SMOS retrievals obtained from the ascending and descending overpasses are then compared to the reference soil moisture data (XAJ SMD). Fig. 6 presents the scatterplots of the XAJ SMD against soil moisture measurements retrieved from the two SMOS observations (the corresponding time series plots of SMOS soil moisture measurements and SMD are in Fig. 4a). As seen in the figure, the lower-left part of the SMOS soil moisture represents the wilting point, and the higher range represents the saturation point of the soil. The values depend on the soil porosity (for saturation) and vegetation cover (for the wilting point). Therefore, they cannot be either near 0 m^3/m^3 or 1 m^3/m^3. In this basin, it is roughly between <0.1 m^3/m^3 and slightly >0.5 m^3/m^3 (for both overpasses), with the descending values generally higher than the ascending observations. For other basins, the range can be different. Each plot includes the linear correlation coefficient r and Spearman correlation coefficient r_{sp}. The results of r and r_{sp} yield similar values, indicating that there is no strong nonlinearity; hence, the linear fitting is suitable to be used in this study. It is clear to see that both overpasses show good correlations with the XAJ-generated surface SMD. Nevertheless, the statistical results reveal that the performance of descending retrievals is better than their ascending counterparts for the whole monitoring period (approximately 10% better). This result is again not as expected and could be partly explained by the fact that this area is highly affected by RFI, which preferentially affects the ascending retrievals because of the SMOS antenna pattern (Collow et al., 2012). The RFI increases the brightness temperature and hence artificially reduces the measured soil moisture (Collow et al., 2012). It is believed that RFI is the main source of error in the SMOS soil moisture products (Chen et al., 2013a). If the RFI emissions are relatively constant, useful corrections could be made in the future (Collow et al., 2012).

In order to examine the development of SMOS soil moisture retrieval ability since the mission commenced, an additional investigation is performed by dividing data into four individual years to determine whether the correlation with the XAJ SMD improved with time. In order to realize this, the scatterplots of the XAJ SMD against four-year SMOS soil moisture data are illustrated in Fig. 7 (the corresponding time series plots of SMOS soil moisture measurements and SMD are in Fig. 4a). Again, the ascending and descending overpasses are evaluated separately. The statistical comparison is shown in Table 2. Generally speaking, there is no sufficient evidence to conclude that the SMOS retrieving algorithm improved with time; in fact, the statistical results indicate that the soil moisture accuracy oscillates every year. This is because the retrieval ability can be influenced by various factors, such as the change of basin conditions (e.g., soil properties change due to agricultural cultivation and vegetation coverage transformation) as well as the maintenance of the instrument itself and the retrieval algorithm used. Similar to the aforementioned conclusion, the performance of the descending orbit surpasses the ascending orbit in most years, and the descending orbit exhibits a relatively steady performance throughout all years (all r are better than –0.63). However, the ascending orbit provides rather unstable results; the performance can vary from r = –0.39 to r = –0.67, and the worst outcomes are discovered in 2011 and 2012.

3.3 Comparison of the SMOS products and SMD based on frozen and unfrozen seasons

Further validation is conducted based on frozen and unfrozen soil conditions. This is because it has been noticed in many previous studies that SMOS evaluation can be difficult when the soil is frozen (Chen et al., 2013b; Collow et al., 2012; Leroux et al., 2014; Panciera et al., 2009). The inaccurate measurements made during winter can affect the overall retrieval quality and are not representative of the SMOS evaluation. For this reason, the soil moisture data are further divided into frozen and unfrozen seasons. Based on the phenomenon discovered in the previous section, the frozen season in the Pontiac Basin is defined as November through February (e.g., based on the pattern of the SMOS soil moisture changes in Fig. 4a, which uses the same method as described by Chen et al. (2013b)) whereas the unfrozen season is represented by the months from March to October. In this section, the results are discussed based on the soil moisture datasets from the whole monitoring period as well as from the four individual years (i.e., 2010 to 2013). As shown in Figs. 8 and 9 (the corresponding time series plots of SMOS

soil moisture measurements and SMD are shown in Fig. 4a), it is evident that the inclusion of frozen soil data can have a significant impact on overall performance, especially on the ascending orbit. Note that the ascending data are not available for the 2010 frozen season. It is observed that for the ascending orbit, the frozen and unfrozen datasets show two rather different relationships with the XAJ SMD (as presented in Fig. 8a). Likewise, the phenomenon is even more dramatic in Fig. 9c, in which the two ascending datasets (i.e., frozen and unfrozen) have completely opposite correlations with the XAJ SMD, which is the only opposite case. The results of all evaluations between the two SMOS overpasses and XAJ SMD in terms of r and r_{sp} values are reported in Table 3 with respect to the whole monitoring period as well as the four individual years. It is obvious that the improvements in both orbits are remarkable. For the ascending overpass, the correlation is increased from $r = -0.53$ to $r = -0.65$, and the poor results discovered previously for 2011 and 2012 are also raised to $r = -0.53$ and $r = -0.58$, respectively. For the descending orbit, the improvement is also significant. The overall correlation rises from $r = -0.62$ to $r = -0.70$, and the results for individual years are also further improved (all r values are better than –0.69). Although the ascending orbit is improved dramatically, the descending orbit is still preferable for hydrological applications. Collow et al. (2012) also found that in northern Oklahoma, U.S., the retrieval from the descending overpass seemed to be more accurate, and they suggested that the ascending overpass was affected by RFI. In contrast, some other studies found that there was no obvious difference between the daytime overpass and the nighttime overpass (Jackson et al., 2012; Sanchez et al., 2012). Based on the results found in this study, it is clear that apart from the RFI influence, the existence of frozen soil can also make a big difference on the soil moisture evaluation outcome. Therefore, it is logical that the conclusion should be derived from the evaluation during the unfrozen season in satellite soil moisture assessment studies.

4. Conclusions

SMOS is the first mission dedicated to monitoring surface soil moisture on a global scale. Depending on the purpose of soil moisture products, the quality of SMOS measurements may vary. Hence, it is vital to evaluate SMOS data based on various application aspects to enable the data developer and end user to better understand the quality and uncertainties of the data and possible ways to improve them. This study investigates the potential

of SMOS Level-3 data in a hydrological application by the XAJ model in a medium-sized basin characterized by cropland and a summer continental climate. Based on our literature review, this is the first study using a three-layer XAJ model with the longest SMOS data records covering both the ascending and descending orbit overpasses.

First, it has been found that both SMOS ascending and descending overpasses demonstrate high variability with seasons and follow a strong seasonal cycle. They correlated reasonably well (r = –0.53 and r = –0.62 for the ascending and descending orbits, respectively) with the XAJ-modeled surface SMD during the whole monitoring period. When the investigation is implemented for each individual year, the result fluctuates; in other words, the SMOS soil moisture retrieving skill did not improve with time as we had expected. The situation for the ascending orbit is even worse than that of the descending orbit, especially in 2011 (r = –0.39) and 2012 (r = –0.48). Second, it is found that none of the soil moisture products provide reliable estimates during the frozen season (November–February), especially for the ascending orbit. By removing frozen datasets, the performance of both overpasses improved remarkably for the whole monitoring period (r = –0.65 and r = –0.70 for the ascending and descending soil moistures, respectively) as well as for the four individual years (r between –0.53 and –0.74 and between –0.69 and –0.73 for the ascending and descending observations, respectively). This leads to the conclusion that SMOS evaluation is unreliable when there is frozen soil. Third, it is interesting to note that SMOS retrievals from the descending overpass are consistently wetter (about 11.7% by volume) than the ascending retrievals, which was not expected. This could be explained by the existence of RFI in this region, which preferentially affects the ascending observations. Generally speaking, the descending orbit shows a stronger potential for improved hydrological predictions. This outcome again contradicts the previous hypothesis from other studies that ascending soil moisture measurements would have better performance than their descending counterparts because at dawn, soil is often in near-hydraulic equilibrium.

The evaluation in this study assumes that the XAJ SMD is reliable according to the flow calibration and validation results ($NSE \geq 0.80$); however, the modelled SMD cannot be considered as the "ground truth". One must keep in mind that the output of a hydrological model can be influenced by the accuracy of model inputs such as

precipitation and ET as well as the flow observations. For this reason, future studies that attempt to assimilate SMOS soil moisture measurements into hydrological models will face various uncertainties which should be assessed from the SMOS data. It must be considered that SMOS retrievals during the frozen season are still poor. Because more information is increasingly available from other sources, there is a scope to improve SMOS performance by considering such information to improve the spatial resolution of soil moisture (e.g., by applying downscaling/data fusion techniques), and better algorithms to employ SMOS Level-1C data should be researched. Although this study is focused on a specific area, the methodology adopted here is general and applicable to other sites. Therefore, it should encourage more studies by the hydrological community to assess the potential application of SMOS satellite soil moisture data in hydrological modelling.

References

Al-Shrafany, D., Rico-Ramirez, M.A., Han, D., Bray, M., 2013. Comparative assessment of soil moisture estimation from land surface model and satellite remote sensing based on catchment water balance. Meteorological Applications 21, 521-534.

Bartholomé, E., Belward, A., 2005. GLC2000: a new approach to global land cover mapping from Earth observation data. International Journal of Remote Sensing 26, 1959-1977.

Beljaars, A.C., Viterbo, P., Miller, M.J., Betts, A.K., 1996. The anomalous rainfall over the United States during July 1993: Sensitivity to land surface parameterization and soil moisture anomalies. Monthly Weather Review 124, 362-383.

Brocca, L., Melone, F., Moramarco, T., 2008. On the estimation of antecedent wetness conditions in rainfall–runoff modelling. Hydrological Processes 22, 629-642.

Calder, I., Harding, R., Rosier, P., 1983. An objective assessment of soil-moisture deficit models. Journal of Hydrology 60, 329-355.

Calvet, J.-C., Wigneron, J.-P., Walker, J., Karbou, F., Chanzy, A., Albergel, C., 2011. Sensitivity of passive microwave observations to soil moisture and vegetation water content: L-band to W-band. Geoscience and Remote Sensing, IEEE Transactions on 49, 1190-1199.

Chen, X., Yang, T., Wang, X., Xu, C.-Y., Yu, Z., 2013a. Uncertainty Intercomparison of Different Hydrological Models in Simulating Extreme Flows. Water resources management 27, 1393-1409.

Chen, Y., Yang, K., Qin, J., Zhao, L., Tang, W., Han, M., 2013b. Evaluation of AMSR-E retrievals and GLDAS simulations against observations of a soil moisture network on the central Tibetan Plateau. Journal of Geophysical Research: Atmospheres 118, 4466-4475.

Collow, T.W., Robock, A., Basara, J.B., Illston, B.G., 2012. Evaluation of SMOS retrievals of soil moisture over the central United States with currently available in situ observations. Journal of Geophysical Research: Atmospheres (1984–2012) 117.

Dai, A., Trenberth, K.E., Qian, T., 2004. A global dataset of Palmer Drought Severity Index for 1870-2002: Relationship with soil moisture and effects of surface warming. Journal of Hydrometeorology 5, 1117-1130.

Daly, C., Neilson, R.P., Phillips, D.L., 1994. A statistical-topographic model for mapping climatological precipitation over mountainous terrain. Journal of applied meteorology 33, 140-158.

Dente, L., Su, Z., Wen, J., 2012. Validation of SMOS soil moisture products over the maqu and twente regions. Sensors 12, 9965-9986.

Engman, E.T., Chauhan, N., 1995. Status of microwave soil moisture measurements with remote sensing. Remote Sensing of Environment 51, 189-198.

Hansen, M., R. DeFries, J.R.G. Townshend, and R. Sohlberg, 1998. UMD Global Land Cover Classification, in: 1 Kilometer, Department of Geography, University of Maryland, College Park, Maryland, 1981-1994 (Ed.).

Jackson, T.J., 1980. Profile soil moisture from surface measurements. Journal of the Irrigation and Drainage Division, American Society of Civil Engineers 106, 81-92.

Jackson, T.J., Bindlish, R., Cosh, M.H., Zhao, T., Starks, P.J., Bosch, D.D., Seyfried, M., Moran, M.S., Goodrich, D.C., Kerr, Y.H., 2012. Validation of Soil Moisture and Ocean Salinity (SMOS) soil moisture over watershed networks in the US. Geoscience and Remote Sensing, IEEE Transactions on 50, 1530-1543.

Jackson, T.J., Cosh, M.H., Bindlish, R., Starks, P.J., Bosch, D.D., Seyfried, M., Goodrich, D.C., Moran, M.S., Du, J., 2010. Validation of advanced microwave scanning radiometer soil moisture products. Geoscience and Remote Sensing, IEEE Transactions on 48, 4256-4272.

Jung, M., Reichstein, M., Ciais, P., Seneviratne, S.I., Sheffield, J., Goulden, M.L., Bonan, G., Cescatti, A., Chen, J., de Jeu, R., 2010. Recent decline in the global land evapotranspiration trend due to limited moisture supply. Nature 467, 951-954.

Kerr, Y.H., Waldteufel, P., Richaume, P., Wigneron, J.-P., Ferrazzoli, P., Mahmoodi, A., Al Bitar, A., Cabot, F., Gruhier, C., Juglea, S.E., 2012. The SMOS soil moisture retrieval algorithm. Geoscience and Remote Sensing, IEEE Transactions on 50, 1384-1403.

Kerr, Y.H., Waldteufel, P., Wigneron, J.-P., Delwart, S., Cabot, F., Boutin, J., Escorihuela, M.-J., Font, J., Reul, N., Gruhier, C., 2010. The smos mission: New tool for monitoring key elements ofthe global water cycle. Proceedings of the IEEE 98, 666-687.

Kerr, Y.H., Waldteufel, P., Wigneron, J.-P., Martinuzzi, J., Font, J., Berger, M., 2001. Soil moisture retrieval from space: The Soil Moisture and Ocean Salinity (SMOS) mission. Geoscience and Remote Sensing, IEEE Transactions on 39, 1729-1735.

Khan, M., 1993. Xinanjiang Model on Bird Creek catchment in USA. Pakistan Journal of Agricultural Research 14, 373-382.

Koster, R.D., Dirmeyer, P.A., Guo, Z., Bonan, G., Chan, E., Cox, P., Gordon, C., Kanae, S., Kowalczyk, E., Lawrence, D., 2004. Regions of strong coupling between soil moisture and precipitation. Science 305, 1138-1140.

Lacava, T., Matgen, P., Brocca, L., Bittelli, M., Pergola, N., Moramarco, T., Tramutoli, V., 2012. A first assessment of the SMOS soil moisture product with in situ and modeled data in Italy and Luxembourg. Geoscience and Remote Sensing, IEEE Transactions on 50, 1612-1622.

Latron, J., Gallart, F., 2008. Runoff generation processes in a small Mediterranean research catchment (Vallcebre, Eastern Pyrenees). Journal of Hydrology 358, 206-220.

Leroux, D.J., Kerr, Y.H., Wood, E.F., Sahoo, A.K., Bindlish, R., Jackson, T.J., 2014. An approach to constructing a homogeneous time series of soil moisture using SMOS. Geoscience and Remote Sensing, IEEE Transactions on 52, 393-405.

Mitchell, K.E., Lohmann, D., Houser, P.R., Wood, E.F., Schaake, J.C., Robock, A., Cosgrove, B.A., Sheffield, J., Duan, Q., Luo, L., 2004. The multi-institution North American Land Data Assimilation System (NLDAS): Utilizing multiple GCIP products and partners in a continental distributed hydrological modeling system. Journal of Geophysical Research: Atmospheres (1984–2012) 109.

Nash, J., Sutcliffe, J., 1970. River flow forecasting through conceptual models part I—A discussion of principles. Journal of Hydrology 10, 282-290.

Njoku, E.G., Jackson, T.J., Lakshmi, V., Chan, T.K., Nghiem, S.V., 2003. Soil moisture retrieval from AMSR-E. Geoscience and Remote Sensing, IEEE Transactions on 41, 215-229.

Ookouchi, Y., Segal, M., Kessler, R., Pielke, R., 1984. Evaluation of soil moisture effects on the generation and modification of mesoscale circulations. Monthly Weather Review 112, 2281-2292.

Panciera, R., Walker, J.P., Kalma, J.D., Kim, E.J., Saleh, K., Wigneron, J.-P., 2009. Evaluation of the SMOS L-MEB passive microwave soil moisture retrieval algorithm. Remote Sensing of Environment 113, 435-444.

Peel, M.C., Finlayson, B.L., McMahon, T.A., 2007. Updated world map of the Köppen-Geiger climate classification. Hydrology and Earth System Sciences Discussions 4, 439-473.

Peng, G., Leslie, L.M., Shao, Y., 2002. Environmental Modelling and Prediction. Springer.

Piles, M., Camps, A., Vall-Llossera, M., Corbella, I., Panciera, R., Rudiger, C., Kerr, Y.H., Walker, J., 2011. Downscaling SMOS-derived soil moisture using MODIS visible/infrared data. Geoscience and Remote Sensing, IEEE Transactions on 49, 3156-3166.

Pinori, S., Crapolicchio, R., Mecklenburg, S., 2008. Preparing the ESA-SMOS (soil moisture and ocean salinity) mission-overview of the user data products and data distribution strategy, Microwave Radiometry and Remote Sensing of the Environment, 2008. MICRORAD 2008. IEEE, Firenze, pp. 1-4.

Prigent, C., Aires, F., Rossow, W.B., Robock, A., 2005. Sensitivity of satellite microwave and infrared observations to soil moisture at a global scale: Relationship of satellite observations to in situ soil moisture measurements. Journal of Geophysical Research: Atmospheres (1984–2012) 110.

Reichle, R.H., Koster, R.D., Dong, J., Berg, A.A., 2004. Global soil moisture from satellite observations, land surface models, and ground data: Implications for data assimilation. Journal of Hydrometeorology 5, 430-442.

Ren-Jun, Z., 1992. The Xinanjiang model applied in China. Journal of Hydrology 135, 371-381.

Rowlandson, T.L., Hornbuckle, B.K., Bramer, L.M., Patton, J.C., Logsdon, S.D., 2012. Comparisons of evening and morning SMOS passes over the Midwest United States. Geoscience and Remote Sensing, IEEE Transactions on 50, 1544-1555.

Rudiger, C., Walker, J.P., Kerr, Y.H., 2011. On the airborne spatial coverage requirement for microwave satellite validation. Geoscience and Remote Sensing Letters, IEEE 8, 824-828.

Rushton, K., Eilers, V., Carter, R., 2006. Improved soil moisture balance methodology for recharge estimation. Journal of Hydrology 318, 379-399.

Sanchez, N., Martinez-Fernandez, J., Scaini, A., Perez-Gutierrez, C., 2012. Validation of the SMOS L2 soil moisture data in the REMEDHUS network (Spain). Geoscience and Remote Sensing, IEEE Transactions on 50, 1602-1611.

Seneviratne, S.I., Corti, T., Davin, E.L., Hirschi, M., Jaeger, E.B., Lehner, I., Orlowsky, B., Teuling, A.J., 2010. Investigating soil moisture–climate interactions in a changing climate: A review. Earth-Science Reviews 99, 125-161.

Spence, C., 2010. A paradigm shift in hydrology: Storage thresholds across scales influence catchment runoff generation. Geography Compass 4, 819-833.

Srivastava, P.K., Han, D., Ramirez, M.A., O'Neil, P., Islam, T., Gupta, M., 2014. Assessment of SMOS soil moisture retrieval parameters using tau-omega algorithms for soil moisture deficit estimation. Journal of Hydrology 519, 574-587.

Srivastava, P.K., Han, D., Ramirez, M.R., Islam, T., 2013a. Machine learning techniques for downscaling SMOS satellite soil moisture using MODIS land surface temperature for hydrological application. Water resources management 27, 3127-3144.

Srivastava, P.K., Han, D., Rico Ramirez, M.A., Islam, T., 2013b. Appraisal of SMOS soil moisture at a catchment scale in a temperate maritime climate. Journal of Hydrology 498, 292-304.

Suseela, V., Conant, R.T., Wallenstein, M.D., Dukes, J.S., 2012. Effects of soil moisture on the temperature sensitivity of heterotrophic respiration vary seasonally in an old-field climate change experiment. Global Change Biology 18, 336-348.

Tromp-van Meerveld, H., McDonnell, J., 2006. Threshold relations in subsurface stormflow: 1. A 147-storm analysis of the Panola hillslope. Water Resources Research 42.

Vinnikov, K.Y., Robock, A., Qiu, S., Entin, J.K., Owe, M., Choudhury, B.J., Hollinger, S.E., Njoku, E.G., 1999. Satellite remote sensing of soil moisture in Illinois, United States. Journal of Geophysical Research: Atmospheres (1984–2012) 104, 4145-4168.

Walker, J.P., Willgoose, G.R., Kalma, J.D., 2004. In situ measurement of soil moisture: a comparison of techniques. Journal of Hydrology 293, 85-99.

Wang, L., Qu, J.J., 2009. Satellite remote sensing applications for surface soil moisture monitoring: a review. Frontiers of Earth Science in China 3, 237-247.

Wang, Q., 1991. The genetic algorithm and its application to calibrating conceptual rainfall-runoff models. Water resources research 27, 2467-2471.

Webb, R.W., Rosenzweig, C.E., Levine, E.R., 2000. Global Soil Texture and Derived Water-Holding Capacities (Webb et al.). Data set. Available on-line [http://www. daac. ornl. gov] from Oak Ridge National Laboratory Distributed Active Archive Center, Oak Ridge, Tennessee, USA.

Western, A.W., Grayson, R.B., 1998. The Tarrawarra data set: Soil moisture patterns, soil characteristics, and hydrological flux measurements. Water Resources Research 34, 2765-2768.

Yeh, T., Wetherald, R., Manabe, S., 1984. The effect of soil moisture on the short-term climate and hydrology change-A numerical experiment. Monthly Weather Review 112, 474-490.

Zhao, R.-J., 1980. The Xinanjiang model, . *Hydrological Forecasting Proceedings Oxford Symposium, IASH 129* 351-356.

Zhao, R.-J., 1992. The Xinanjiang model applied in China. Journal of Hydrology 135, 371-381.

Zhao, R.-J., Liu, X., Singh, V., 1995. The Xinanjiang model. Computer models of watershed hydrology., 215-232.

Zhuo, L., Dai, Q., Han, D., 2014. Meta-analysis of flow modeling performances—to build a matching system between catchment complexity and model types. Hydrological Processes, 29: 2463-2477.

Zhuo L, Han D, Dai Q, Islam T, Srivastava PK. 2015. Appraisal of NLDAS-2 Multi-Model Simulated Soil Moistures for Hydrological Modelling. Water Resources Management: 1-15. DOI: 10.1007/s11269-015-1011-1.

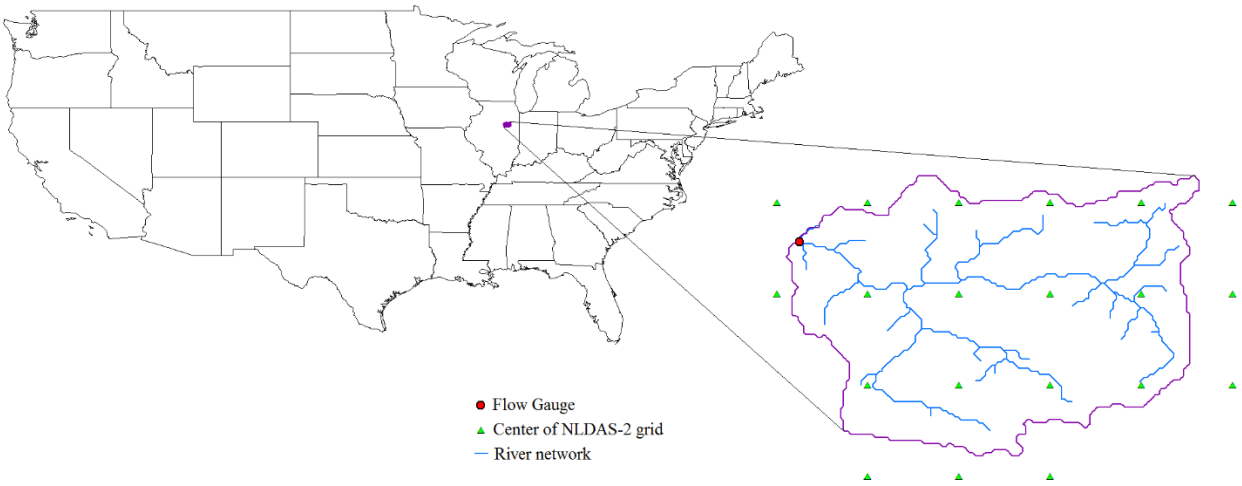

Fig. 1. Locations of the Pontiac basin with the flow gauge and NLDAS-2 grid points over the river network.

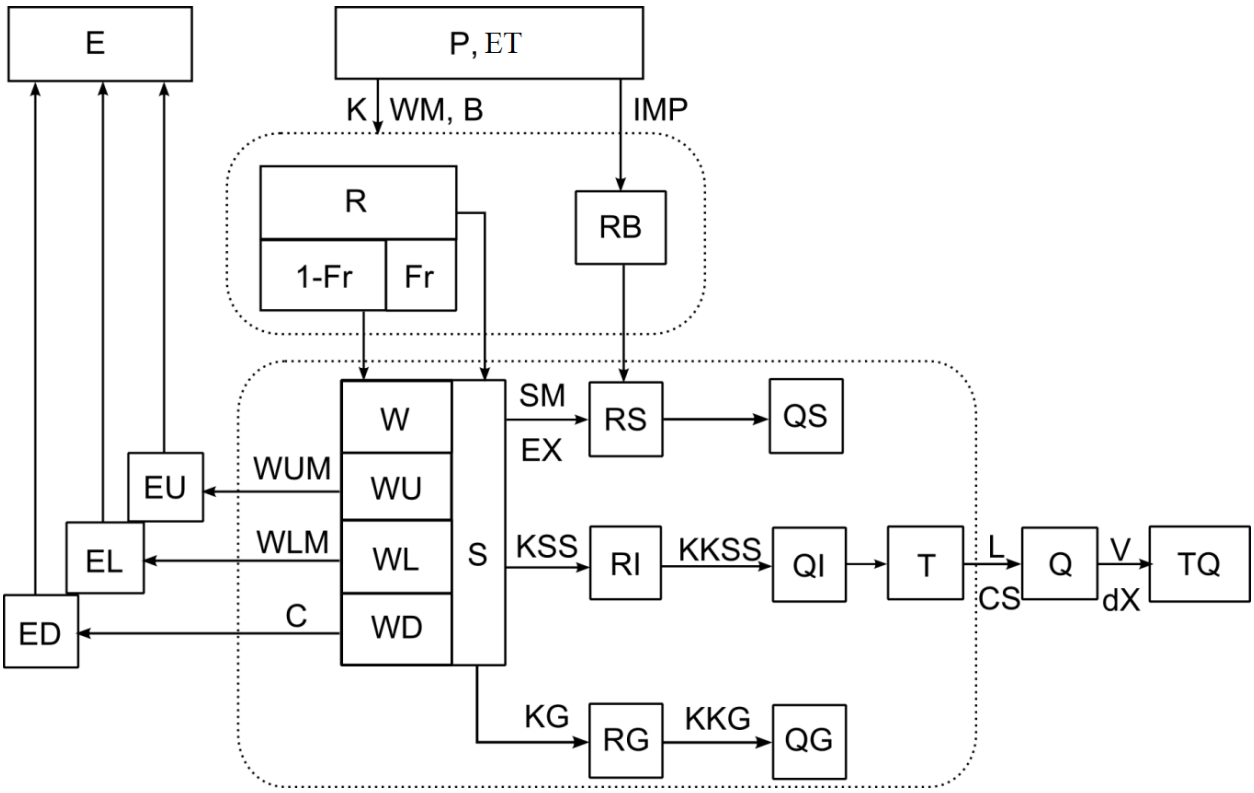

Fig. 2. Flowchart of the XAJ model (Zhao, 1992), where *W* is the areal mean tension water storage with three components *WU*, *WL*, and *WD*, representing upper, lower, and deep soil layers, respectively; *S* is the areal mean free water storage; *Fr* is the factor of runoff producing area related to *W*; *IMP* is the factor of impervious area in a basin; *RB* is the direct runoff produced from the small portion of impervious area; and *R* is the total runoff generated from the model with surface runoff (*RS*), interflow (*RI*), and groundwater runoff (*RG*) components, respectively. These three runoff components are then transferred into *QS*, *QI*, and *QG* and combined as the total sub-basin inflow (*T*) to the channel network. The flow outputs *Q* from each sub-basin are then routed to the basin outlet to produce the final flow result (*TQ*).

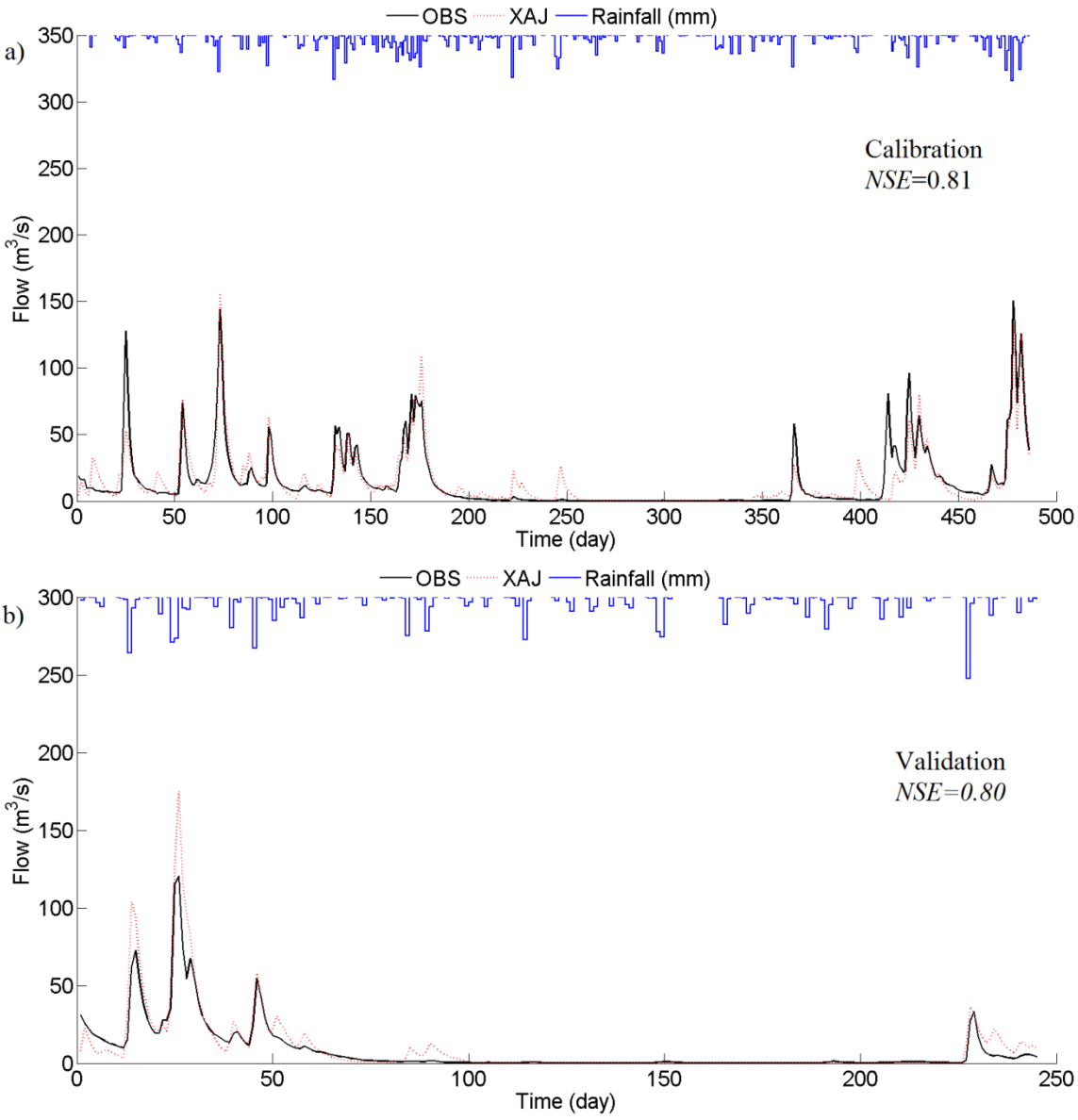

Fig. 3. Time series of daily rainfall and daily average flow for the Pontiac basin during calibration (a) and validation (b) periods.

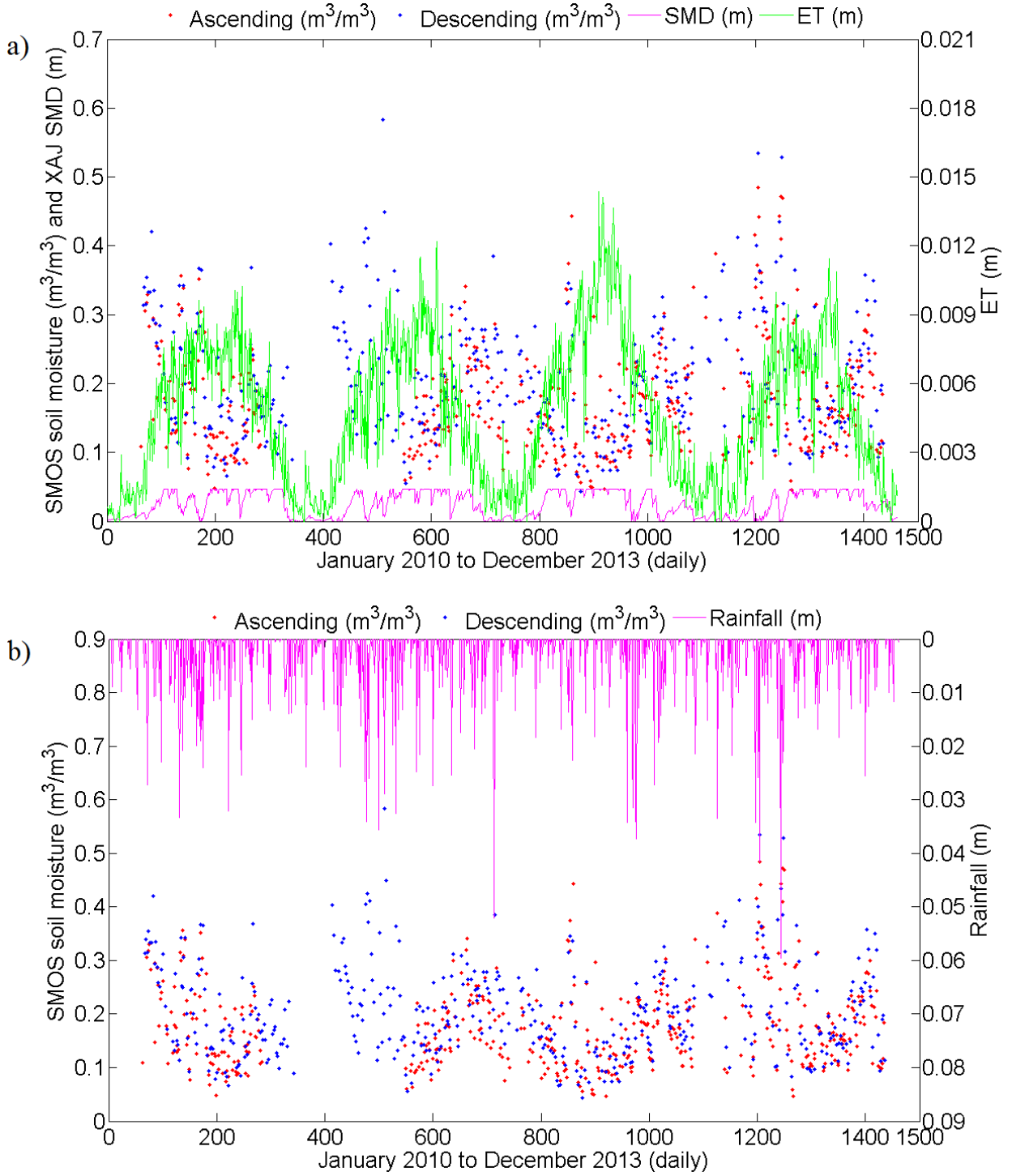

Fig. 4. Time series of the SMOS soil moistures (both ascending and descending orbits) and XAJ surface SMD with ET (a) and with rainfall (b). The total numbers of observations for the ascending and descending overpasses are 464 and 432 days, respectively, during the whole monitoring period.

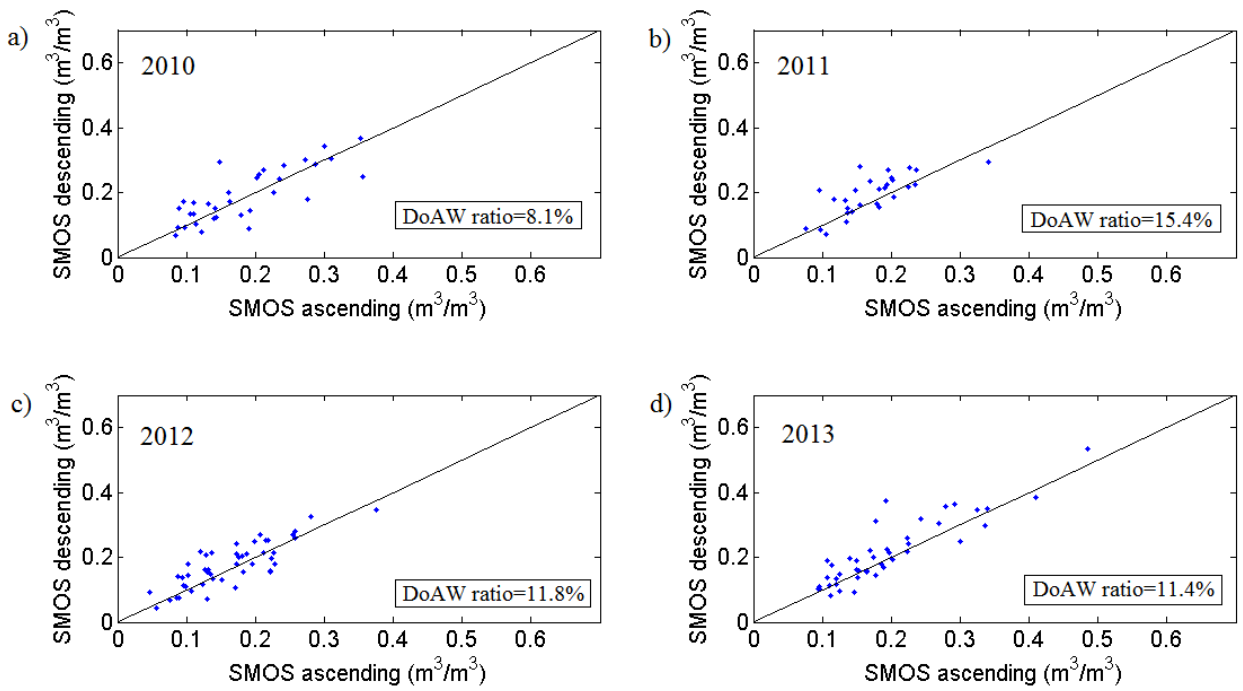

Fig. 5. Scatterplots of the SMOS descending soil moistures against the ascending retrievals, with descending-over-ascending-wetting ratio (DoAW ratio; i.e., the difference between the descending and ascending soil moistures divided by the ascending soil moisture) presented in each year.

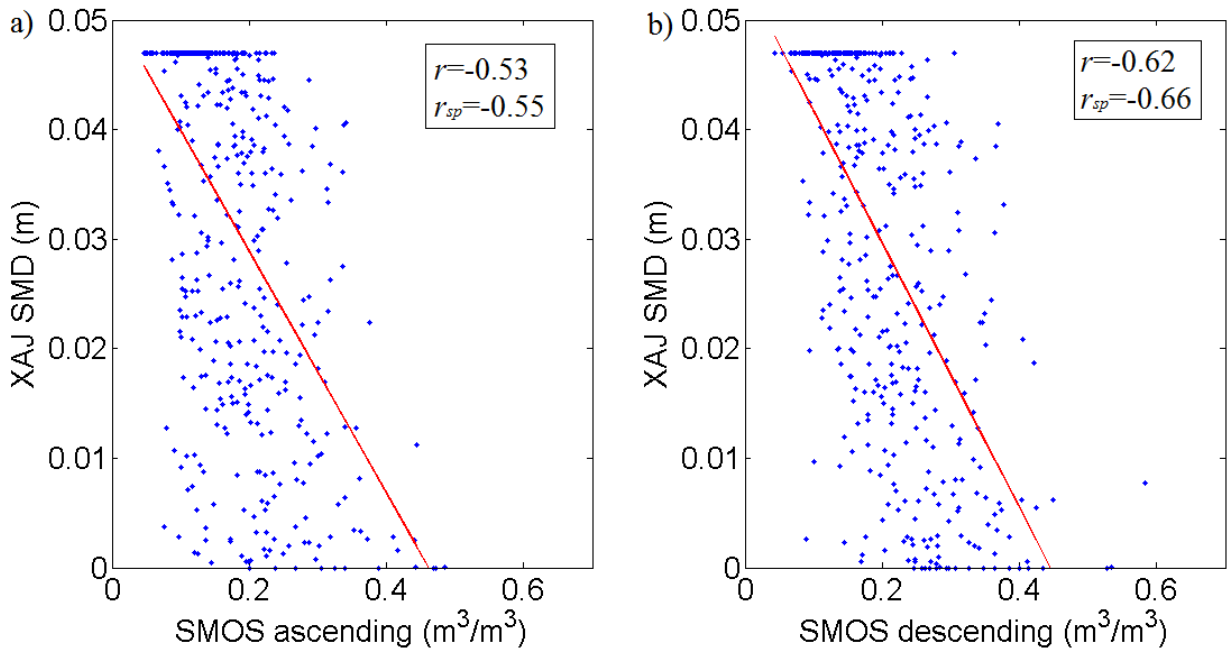

Fig. 6. Scatterplots of the XAJ surface SMD against soil moistures from the two SMOS footprints: (a) ascending and (b) descending during the whole monitoring period.

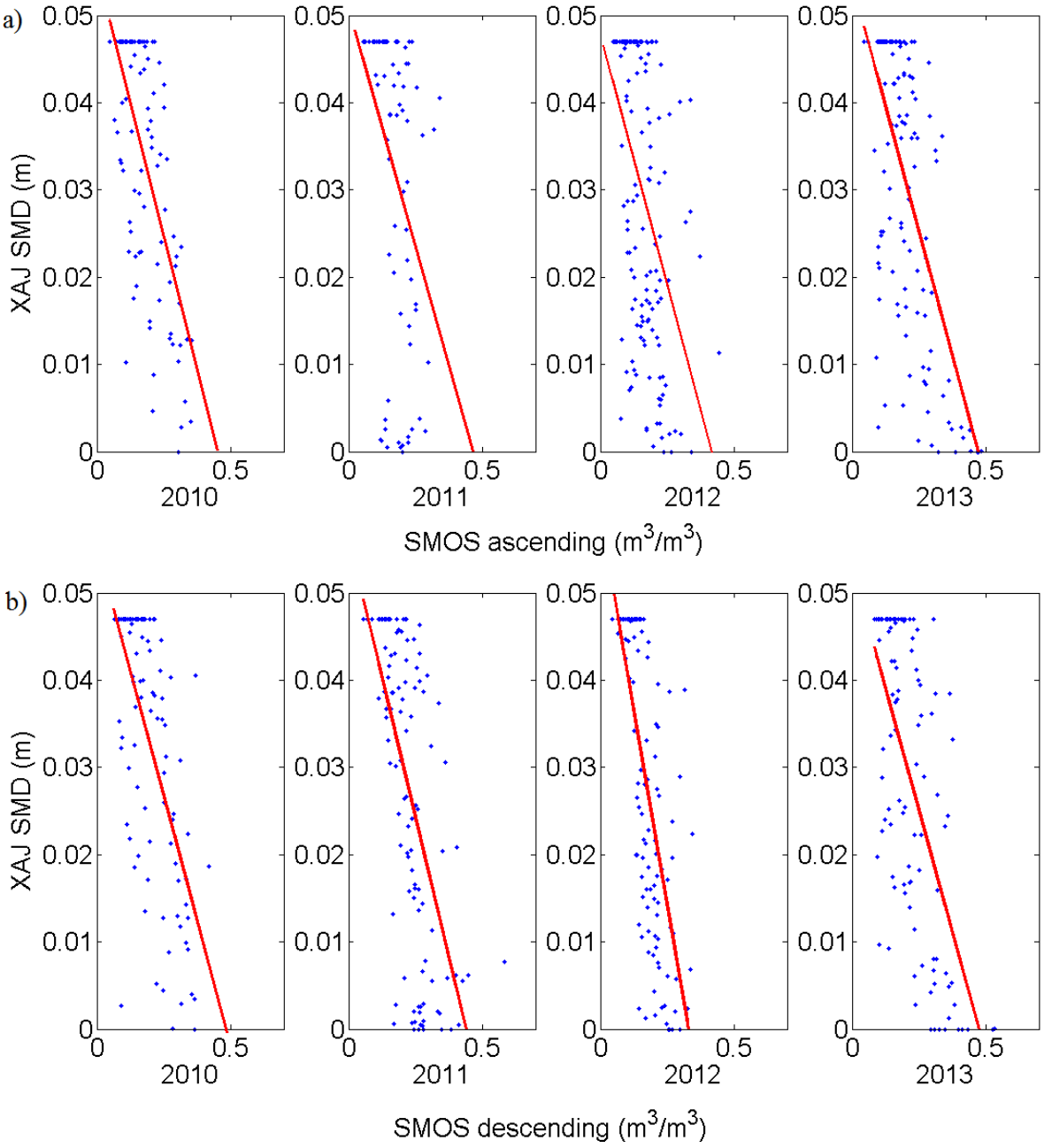

Fig. 7. Scatterplots of the XAJ surface SMD against the four-year SMOS soil moistures, shown in the order of (a) ascending and (b) descending overpasses.

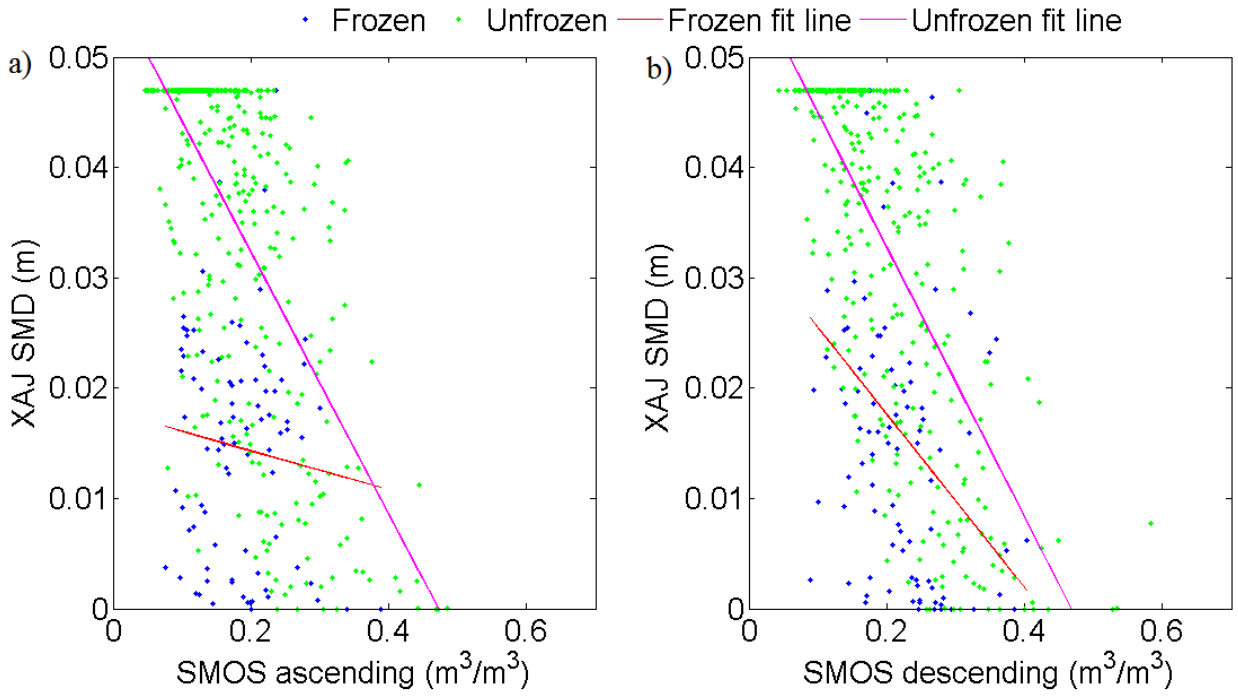

Fig. 8. Scatterplots of the XAJ surface SMD against the soil moistures from the two SMOS overpasses: (a) ascending and (b) descending. The analysis is based on frozen and unfrozen seasons.

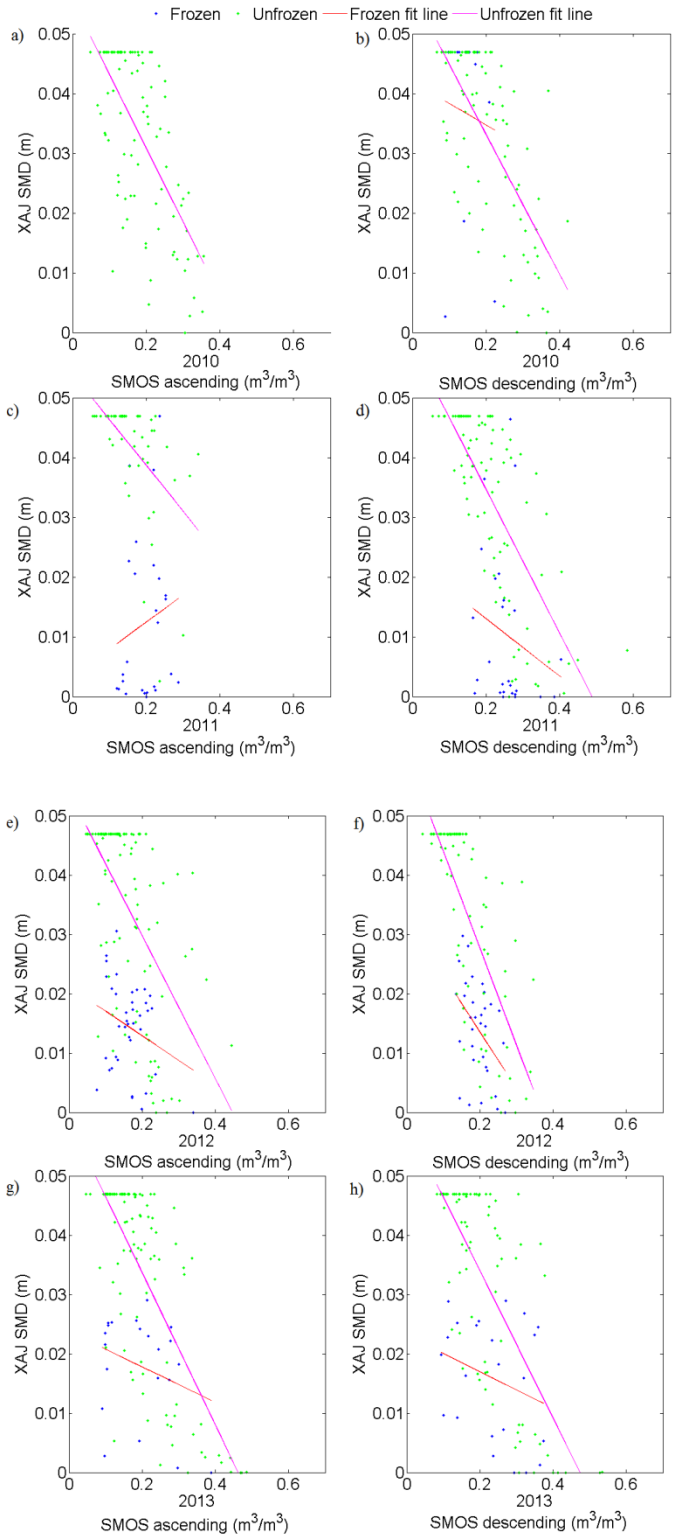

Fig. 9. Scatterplots of the XAJ surface SMD against the four-year (i.e., 2010 to 2013) soil moistures from the two SMOS overpasses: (a) ascending and (b) descending. The analysis is based on frozen and unfrozen seasons. Note that the ascending data is not available in the frozen season in 2010.

Table 1. The XAJ model parameters used in the Pontiac basin.

Symbol	Model parameters	Unit	Optimal value	Range
K	Ratio of potential evapotranspiration to pan evapotranspiration	[-]	0.56	0.10-1.20
SM	Areal mean free water capacity of the surface soil layer, which represents the maximum possible deficit of free water storage	mm	31.48	10-50
KG	Outflow coefficients of the free water storage to groundwater relationships	[-]	0.10	0.10-0.70
KSS	Outflow coefficients of the free water storage to interflow relationships	[-]	0.19	0.10-0.70
KKG	Recession constants of the groundwater storage	[-]	0.31	0.01-0.99
KKSS	Recession constants of the lower interflow storage	[-]	0.01	0.01-0.99
CS	Recession constant in the lag and route method for routing through the channel system with each sub-basin	[-]	0.26	0.10-0.70
WUM	Averaged soil moisture storage capacity of the upper layer	mm	46.96	30-50
WLM	Averaged soil moisture storage capacity of the lower layer	mm	39.08	20-150
WDM	Averaged soil moisture storage capacity of the deep layer	mm	30.11	30-400
IMP	Percentage of impervious and saturated areas in the catchment	%	0.00	0.00-0.10
B	Exponential parameter with a single parabolic curve, which represents the non-uniformity of the spatial distribution of the soil moisture storage capacity over the catchment	[-]	0.70	0.10-0.90
C	Coefficient of the deep layer that depends on the proportion of the basin area covered by vegetation with deep roots	[-]	0.49	0.10-0.70
EX	Exponent of the free water capacity curve influencing the development of the saturated area	[-]	1.93	1.10-2.00
L	Lag in time	[-]	0.00	0.00-6.00
V	Parameter of the Muskingum method	m/s	0.43	0.40-1.20
dX	Parameter of the Muskingum method	[-]	0.18	0.00-0.40

Table 2. Statistical performance of the four-year SMOS estimated soil moistures (both ascending and descending overpasses) against the XAJ surface SMD in the Pontiac basin.

	r		r_{sp}	
	Ascending	Descending	Ascending	Descending
2010	-0.67	-0.63	-0.63	-0.59
2011	-0.39	-0.63	-0.54	-0.69
2012	-0.48	-0.70	-0.55	-0.74
2013	-0.65	-0.64	-0.59	-0.63

Table 3. Statistical indicators of the four-year SMOS estimated soil moistures in frozen and unfrozen seasons for the Pontiac catchment.

		r		r_{sp}	
		Ascending	Descending	Ascending	Descending
Frozen	2010	--	-0.09	--	-0.14
	2011	0.16	-0.21	0.22	-0.35
	2012	-0.27	-0.43	-0.20	-0.43
	2013	-0.29	-0.28	-0.19	-0.27
	All Four years	-0.11	-0.39	-0.13	-0.45
Unfrozen	2010	-0.67	-0.69	-0.63	-0.65
	2011	-0.53	-0.72	-0.66	-0.75
	2012	-0.58	-0.73	-0.63	-0.76
	2013	-0.74	-0.73	-0.70	-0.70
	All Four years	-0.65	-0.70	-0.64	-0.70